

EVALUATION OF CONDITIONAL MEAN SPECTRA CODE CRITERIA FOR GROUND MOTION SELECTION

Tamika J. Bassman, A.M.ASCE, Kuanshi Zhong, Jack W. Baker, M.ASCE

August 29, 2022

Abstract

The choice of spectral targets for ground motion selection has a strong impact on structural demands resulting from nonlinear time history analysis. In particular, the conditional mean spectrum (CMS) has been recognized as an appealing alternative to the uniform hazard spectrum (UHS) as a spectral target due to the former's more realistic shape and reduced conservatism. Using a tall building case study in a high-seismicity region, this paper evaluates the building demands generated by UHS- and CMS-based selection procedures. Theoretically rigorous implementation of CMS-based selection using 17 different conditioning periods is shown to reduce maximum considered earthquake (MCE)-level demands on the case study building by 9-35% relative to UHS-based selection. Furthermore, the simplified CMS-based procedure codified in ASCE 7-22 with apt choice of only two conditioning periods is found to satisfactorily capture the demands generated by the theoretically rigorous approach. Findings also highlight the degree of sensitivity of CMS-based results to the choice of conditioning periods and to enforcement of lower bounds on spectral targets, such as 75% of the UHS. The presented analysis procedure can be replicated in future studies for explicit evaluation of simplified CMS ground motion selection in other structural systems or analysis cases.

Practical Applications

Since its introduction to the building code in ASCE 7-16, the alternative, conditional mean spectrum-based method for ground motion selection has gained traction among practitioners due to its reduced conservatism relative to traditional selection methods. To simplify the implementation of conditional mean spectra in practice, the building code alternative method requires a minimum of only two target spectra be used, so long as their envelope satisfies a lower bound within a specified period range. However, there are few quantitative studies of the impacts of these simplifications on the resulting building demands. In this study, we demonstrate how building demands vary when a tall building in a high-seismicity region is analyzed using either a traditional or a conditional mean spectrum-based selection approach. We find that using two reasonable target spectra in accordance with the ASCE 7 alternative method produces acceptable building demands as compared to the demands obtained from performing exhaustive nonlinear analysis with a large number of target spectra. Furthermore, we illustrate how different choices of conditional mean spectrum targets maximize different types of building demands (e.g., interstory drift, base shear, floor acceleration) and how some types of demands are more sensitive to this choice than others. This work provides a procedure for evaluating conditional mean spectrum-based ground motion selection that can be replicated in the future for other buildings or structural systems.

1 Introduction

Ground motion record selection is a key step in performing nonlinear response history analysis of structures for seismic design applications, and has expanded in use in design practice with the continued growth of computational resources and efficiency. The conditional mean spectrum (CMS) is a target spectrum for ground motion selection (Baker and Cornell, 2006; Baker, 2011) and an alternative to the uniform hazard spectrum (UHS), which approximates the spectral shape of building code design spectra when the latter's deterministic cap is not applied. The UHS constitutes an envelope across all periods of spectral acceleration (Sa) values which have a specified exceedance probability (e.g., 2% in 50 years) and is typically calculated by performing site-specific probabilistic seismic hazard assessment (PSHA). Because it is unlikely for spectral amplitudes of equally rare exceedance probability to occur at all periods simultaneously in a single ground motion record, the UHS tends to overestimate structural demands relative to those obtained using alternate approaches such as the CMS.

In contrast, the spectral amplitude of a CMS is only imposed at a single conditioning period (T^*). $Sa(T^*)$ commonly is taken to match the UHS ordinate at T^* , as shown in Fig. 1 for the examples of CMS with $T^* = 1$ s and $T^* = 5$ s, and is obtained from PSHA, which also provides mean values of magnitude M and distance R from hazard disaggregation. The spectral ordinates of the CMS at all other periods T are log-mean values conditioned on $Sa(T^*)$ and rupture characteristics M and R :

$$\mu_{\ln Sa(T)|\ln Sa(T^*)} = \mu_{\ln Sa}(M, R, T) + \rho(T, T^*)\varepsilon(T^*)\sigma_{\ln Sa}(M, R, T) \quad (1)$$

The log-mean $\mu_{\ln Sa}$ and log-standard deviation $\sigma_{\ln Sa}$ in (1) are obtained using a ground motion model (e.g., (e.g., Gregor et al., 2014), and the correlation coefficient $\rho(T, T^*)$ can be obtained from some ground motion models or from a dedicated study (e.g., Baker and Jayaram, 2008). All of those models are usually calibrated using past ground motion recordings. The residual $\varepsilon(T^*)$ captures the difference between $\ln Sa(T^*)$ and the mean $\ln Sa$ value at T^* predicted by the ground motion model:

$$\varepsilon(T^*) = \frac{\ln Sa(T^*) - \mu_{\ln Sa}(M, R, T^*)}{\sigma_{\ln Sa}(M, R, T^*)} \quad (2)$$

Fig. 1 illustrates the residual $\varepsilon(T^* = 5$ s) in relation to the example CMS with $T^* = 5$ s and the predicted median spectrum computed using Boore et al. (2014) with rupture characteristics M and R from hazard disaggregation corresponding to a period of 5s.

Compared with the corresponding UHS, conditional mean spectra have been shown to better approximate the shape of individual ground motion response spectra with identical $Sa(T^*)$, M , and R (Baker, 2011). However, estimating structural demands associated with a given probability of exceedance theoretically requires performing ground motion selection for a large number of CMS targets with T^* covering the full range of possible T , because the critical excitation periods may not be known a priori (Loth and Baker, 2015). To lessen computational demands in design practice while also maintaining the integrity of the procedure, simplifying modifications to the CMS-based ground motion selection approach have been set forth in the building code and by researchers.

The CMS-based method in ASCE 7-22 (2022) requires a minimum of two different target spectra in each orthogonal direction whose T^* are chosen based on the dynamic properties of the structure under consideration. For each CMS target, $Sa(T^*)$ must meet or exceed the spectral ordinate of the risk-targeted maximum considered earthquake (MCE_R) spectrum (approximately the UHS) at T^* . To ensure sufficiently high spectral amplitude at periods other than T^* , the envelope of all CMS targets must meet or exceed 75% of the MCE_R spectrum within a period range for spectral fitting. Generally, the upper bound of this period range (T_{UB}) is twice the value of the largest fundamental period of the building in any principal horizontal direction, and the lower bound (T_{LB}) is the lesser of 20% of the smallest fundamental period and

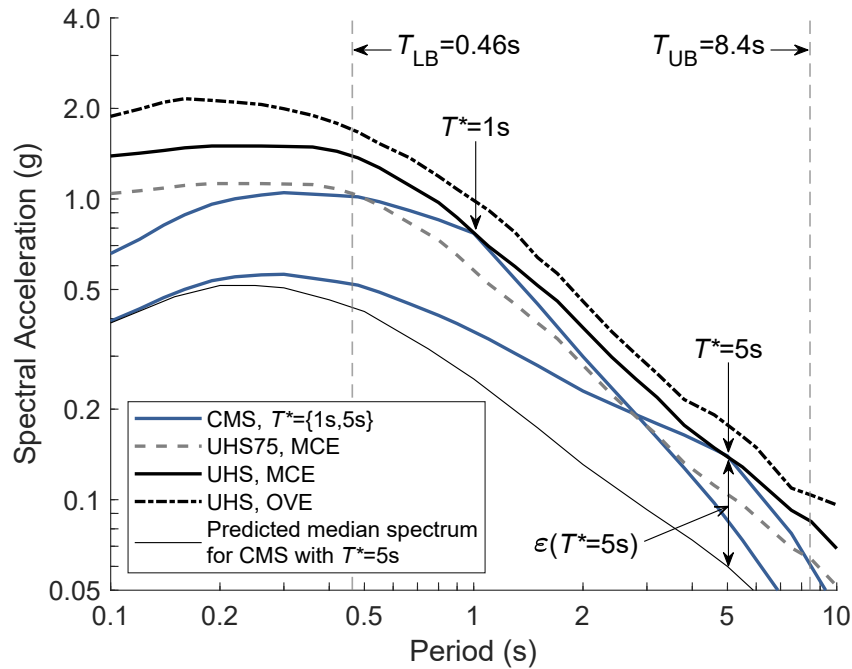


Fig. 1. Examples of target spectra used in this study, with key attributes indicated.

the period needed to achieve 90% mass participation in each principal horizontal direction. Satisfaction of this lower-bound criterion typically requires an artificial increase in spectral ordinates of the original CMS, an additional CMS, or both.

An alternative set of modifications for CMS-based ground motion selection has been proposed by Carlton and Abrahamson (2014), who instead recommend a lower bound of 90% of the UHS for the envelope of all CMS targets and do not specify a period range for spectral fitting. The authors further provide rules for how CMS should be modified to meet the 90% lower-bound criterion. Specifically, they suggest a symmetric broadening of each CMS target about its T^* , with this broadening extending halfway in log space to each adjacent target's respective T^* . Other researchers have proposed other types of target spectra or criteria to address practical implementation of CMS-based ground motion selection. These include amplitude-scaling limits when compensating for insufficient high-amplitude ground motion records (Du et al., 2019) and a generalized CMS-based target spectrum which conditions on Sa values at multiple periods to account for modal separation while reducing the number of targets required (Loth, 2014; Kwong and Chopra, 2017; Kishida, 2017).

In spite of the greater complexity in its implementation, researchers and practitioners alike have noted the potential advantages of a CMS-based approach to ground motion selection in a variety of different seismic applications due to reduced conservatism and greater realism in the ground motions selected and the demands resulting from the procedure. Engineers of a new gravity seawall located in Seattle, Washington, performed nonlinear analyses of the structure using UHS- and CMS-based ground motion selection with three conditioning periods. They reported that an approximately 40% greater wall thickness was required when using the UHS-based procedure, which would equate to several million dollars in added construction costs (Christie and Zhang, 2016). A site-specific seismic hazard analysis of a Mississippi River crossing 200 km away from the New Madrid seismic zone found that liquefaction-induced demands predicted by a CMS-based ground motion selection procedure were more rational and more consistent with historical and geologic precedent than those produced by a UHS-based procedure (Hashash et al., 2013). Performance-

based seismic design procedures for tall buildings, such as those published by PEER (2017) and the Los Angeles Tall Buildings Structural Design Council (2020), recommend use of CMS-based ground motion selection over the traditional UHS-based procedure. Anecdotal evidence has reported notable reduction in building base shear, up to 20% in some cases, when these recommendations are followed.

Although several examples of lowered structural demands obtained using CMS-based target spectra exist, few studies have investigated the nature and extent of the differences in demands resulting from CMS- and UHS-based ground motion selection. A recent study by Arteta et al. (2022) considered the effects of using CMS targets instead of a UHS target and varying the CMS conditioning period on building response estimates. Their study was primarily based on shorter buildings, and did not consider compliance with code requirements in the way that this study does. In particular, the efficacy of simplifying code provisions such as the 75% lower bound prescribed by ASCE 7-22 has yet to be demonstrated, in terms of ability to capture the true structural demands which would be produced by an exhaustive set of CMS targets.

We address the aforementioned issues in the context of a tall building case study located in a high-seismicity region. We first estimate its engineering demand parameters (EDPs) using ground motions selected to match a UHS target. We then compare these demands with those generated by a rigorous implementation of CMS-based record selection, in which a large number of CMS targets covering a broad range of T^* is used. Having determined this theoretical CMS demand baseline, we then evaluate the ability of more practical, simplified CMS procedures (i.e., ASCE, 2022; Carlton and Abrahamson, 2014) to reproduce these baseline results. Based on these findings, we offer further suggestions for effective implementation of CMS in practice, including commentary on the selection of conditioning period, the range of periods prescribed as relevant to the ground motion selection process, and the choice of lower bound enforced on the envelope of the target spectra.

2 Analysis Procedure

2.1 Case Study Building

Tall buildings constitute a class of structure for which CMS-based ground motion selection has particular relevance due to codified requirements and growing use among structural designers. As such, we consider here a 42-story reinforced concrete core wall building located in Los Angeles, California. This structure was originally developed as building 1C in the Task 12 report of the PEER Tall Buildings Initiative (TBI) (Moehle et al., 2011) and designed to meet performance-based design criteria at 2475- and 43-year return period shaking levels.

Fig. 2 illustrates the two-dimensional analysis model of the building, which was prepared and analyzed using OpenSees (McKenna et al., 2010). In this study, we idealized the C-shaped wall in the weak-axis direction using a force-based fiber element model. Each story has one fiber-based element with six integration points, and each integration point aggregates one fiber section and one elastic shear section. The gravity system is modeled by a leaning column to capture $P-\Delta$ effects. The total seismic weight computed from tributary area is 200 MN. Further modeling details are provided in Zhong et al. (2021). Table 1 lists the first five natural periods and corresponding cumulative mass participation for the structural model. Per ASCE 7-22 criteria, the period range of spectral fitting during ground motion selection shown in Fig. 1 is bounded from below at $T_{LB} = 0.46$ s, which corresponds with the third mode of the structure at which 90% mass participation is achieved, and from above at $T_{UB} = 8.4$ s, which is twice the first mode period.

2.2 Seismic Hazard and Target Spectra

The building model was subjected to suites of ground motions corresponding to four different sets of target spectra at each of two return periods of shaking intensity: 2475 (MCE) and 4975 (overdesign earthquake,

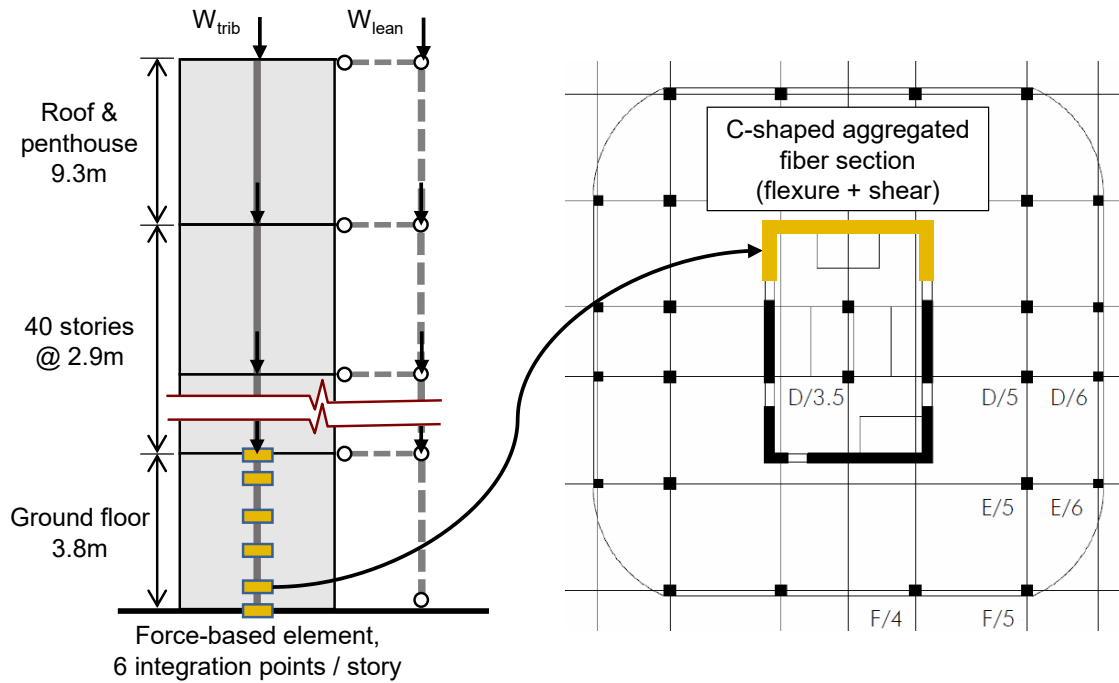


Fig. 2. Diagram of the case study building model, in elevation (left) and section (right). (Figure adapted from Zhong et al. (2021). Story plan view at right adapted from Moehle et al. (2011).)

Table 1. Modal properties of the case study building.

| Mode Number | Period (s) | Cumulative Mass Participation (%) |
|-------------|------------|-----------------------------------|
| 1 | 4.22 | 62 |
| 2 | 0.96 | 84 |
| 3 | 0.46 | 92 |
| 4 | 0.31 | 94 |
| 5 | 0.23 | 96 |

Table 2. Disaggregation data for the approximate building location at 34.050°N, -118.251°W for Site Class C and MCE (2475-year) hazard level, obtained from 2014 National Seismic Hazard Model (Petersen et al., 2015).

| Period (s) | Distance to Rupture (km), R | Magnitude, M | Epsilon, ϵ |
|------------|-------------------------------|----------------|---------------------|
| 0.01 | 8.82 | 6.94 | 1.31 |
| 0.2 | 9.11 | 6.93 | 1.33 |
| 1 | 10.36 | 7.14 | 1.25 |
| 3 | 14.74 | 7.37 | 1.30 |
| 5 | 20.57 | 7.55 | 1.31 |
| 7.5 | 48.11 | 7.75 | 1.33 |
| 10 | 95.78 | 7.88 | 1.33 |

or OVE). Discussion herein focuses primarily on MCE results due to the prevalent use of this hazard level in design practice, including when nonlinear response history analysis is required by code. We utilize the beyond-code OVE hazard level to demonstrate how CMS-based ground motion selection performs in a more extreme case, as the higher amplitudes produce more pointed CMS shapes and thereby a sharper departure from the corresponding UHS. OVE results exhibit similar trends to the corresponding MCE results and are illustrated in the supplemental materials accompanying this paper.

The first set of spectral targets consists of a UHS at either the MCE or OVE level, as shown in Fig. 1. These UHS are taken to match those provided in the TBI Task 12 report (Moehle et al., 2011) for consistency with the analysis used in the design of the original building. The second target set ("Theoretical Procedure") is comprised of 17 CMS with T^* ranging from 0.15s to 9s. The large number of distinct targets in this exhaustive set is intended to establish a theoretical baseline for the building demands that would be produced by a thorough implementation of CMS-based ground motion selection in the absence of time or computational constraints. The remaining two target sets ("Practical Procedures") have reduced computational demands intended for feasibility in design practice. Each procedure comprises only two CMS targets that are modified to meet one of two frameworks for target spectra criteria, either ASCE 7-22 or Carlton and Abrahamson (2014) ("C&A-14"). One such pair of CMS satisfying ASCE 7-22 requirements at MCE is shown in Fig. 1. Comparison of these two sets of practical provisions illustrates the effect of enforcing slightly greater conservatism in target spectral amplitudes, as recommended by C&A-14, than is currently required by code. The CMS in the latter three target sets were initially constructed following the steps described in Baker (2011) using PSHA disaggregation data obtained from the 2014 USGS National Seismic Hazard Model (2015), as listed in Table 2 for the MCE hazard level and Table S1 of the supplemental materials for the OVE hazard level. Additional artificial adjustments were made to CMS used in the two practical procedures as needed to satisfy their respective target spectra criteria.

2.3 Ground Motion Selection and Structural Analysis

Ground motion record selection for all four sets of spectral targets in this study was performed using the algorithm introduced by Baker and Lee (2018) using a subset of the NGA-West2 database (Bozorgnia et al., 2014). For each target spectrum, 40 ground motions were selected and scaled to match the target, as shown in Fig. 3(a). Suites of 40 are used instead of the 11 required by ASCE 7-22 in order to obtain more stable estimates of building demands than are achieved using smaller sets of records. Ground motions were selected from seismic conditions that loosely matched the disaggregation information for the case study building location. The vertical component of motion was excluded from all record selection and analysis.

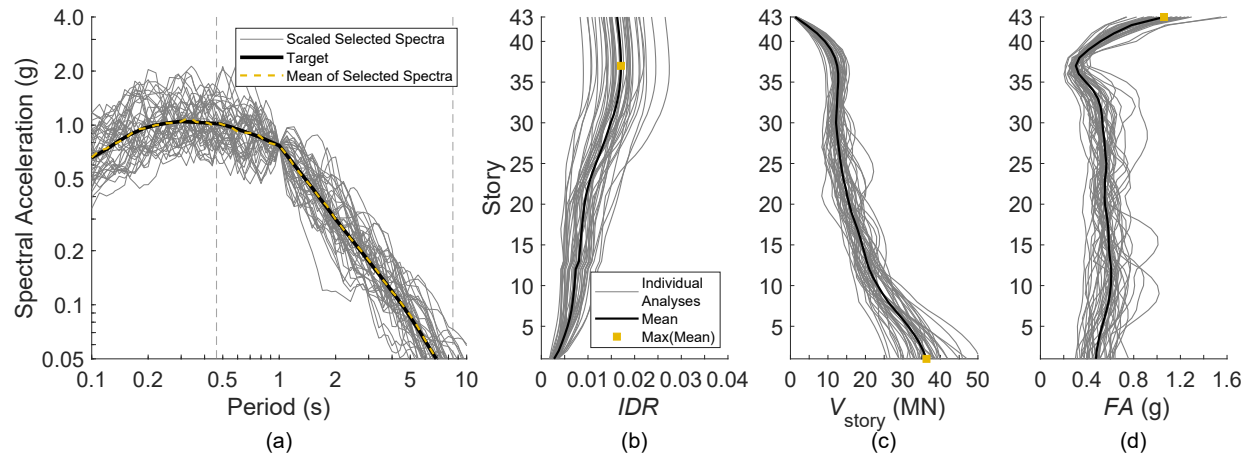


Fig. 3. Results of ground motion selection and nonlinear response history analysis for CMS target with $T^* = 1$ s: (a) spectral target and individual selected spectra; (b)-(d) peak EDPs generated at each story.

The maximum amplitude-scaling factor allowed for selected ground motion records was 5. Additional algorithm parameters used in selection are provided in Table S2 of the supplemental materials.

The following steps were taken to determine the building demands generated by each individual target spectrum within each set of targets. Nonlinear response history analysis was performed on the structural model using each target's selected suite of 40 records. For each ground motion, envelopes of structural response over the building height were generated by recording peak values of three different engineering demand parameters (EDPs) at each story: interstory drift ratio (IDR), story shear (V_{story}), and floor acceleration (FA). These EDPs were selected to collectively capture the effects of both short- and long-period excitation of the structure, in order to check whether a range of EDPs are accurately estimated by a given set of target spectra. For each of the three EDPs, the 40 envelopes over the building height were averaged at each story, as shown by the heavy lines in each of Fig. 3(b)-(d). The maximum value across all stories of each average EDP curve was computed, as indicated by the square markers in each of the same sub-figures. In the ensuing discussion, these demarcated maximum values are considered the governing demands on the structure generated by each target spectrum. For the case study building, the maximum story shear demand is equivalent to the base shear and the maximum floor acceleration demand is consistently at the roof level. As shown in Fig. 3(b)-(d), for the CMS target with $T^* = 1$ s, the governing demands are as follows: interstory drift ratio (IDR_{max}) of 1.71%, base shear ($V_{\text{base,max}}$) of 36.3 MN, and roof acceleration (RA_{max}) of 1.06g.

3 Theoretical CMS Procedure

3.1 Results

The theoretical CMS procedure for ground motion selection uses 17 unmodified CMS target spectra with T^* ranging from 0.15s to 9s and $Sa(T^*)$ at the MCE hazard level. The full set of target spectra, as well as the corresponding MCE UHS, are shown in Fig. 4(a). This set of target spectra, in addition to the use of a suite of 40 ground motions per target, is intended to represent a rigorous implementation of CMS-based ground motion selection which encompasses a comprehensive range of distinct T^* and the building demands consequently generated. While these suites and spectra are technically compliant with the requirements of ASCE 7-22, they would not be used in practice due to the large analysis burden of considering 40 ground motions per each of 17 spectra rather than the minimum of 11 motions for each of 2 spectra required by the code. The analytical procedure for ground motion selection, nonlinear response history analysis, and

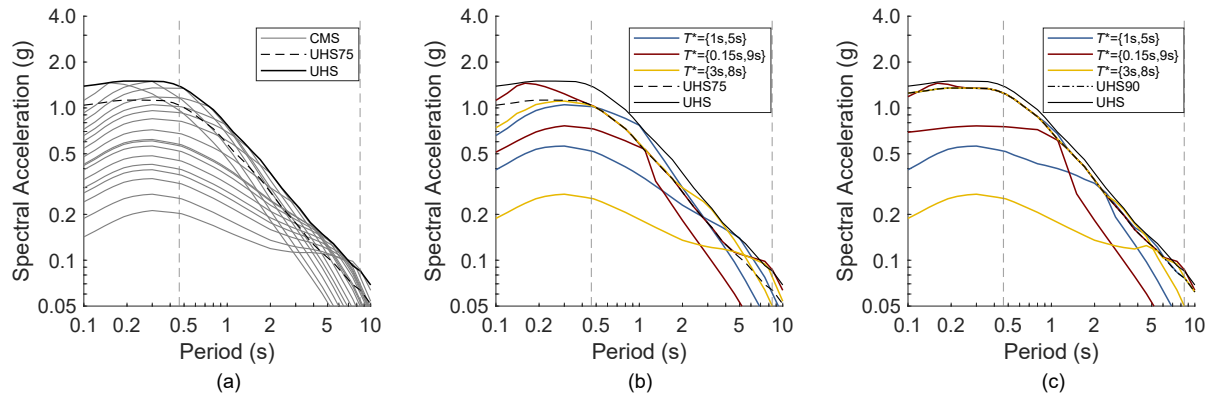


Fig. 4. CMS-based target spectra sets for different ground motion selection procedures: (a) theoretical CMS, (b) ASCE 7-22, (c) C&A-14. UHS-based spectra shown for reference.

calculation of building demands described in the previous section was performed for each individual target spectrum. Fig. 5 summarizes the resulting building demands for the theoretical set of 17 CMS target spectra, for each of the three EDPs of study. Analogous results from analyses performed at the OVE hazard level are shown in Fig. S1 of the supplemental materials. In the ensuing discussion, Fig. 5 and subsequent figures of identical format are referred to as "EDP spectra." Each square marker represents the governing demand, as defined at the end of the previous section, which was generated by the CMS target spectrum whose T^* is the abscissa of the marker. For example, the CMS with a conditioning period of 1s generated governing demands of 1.71% interstory drift, 36.3 MN base shear, and 1.06g roof acceleration as shown in Fig. 3(b)-(d), and these demands are plotted accordingly at $T^* = 1s$ in Fig. 5. The vertical dashed lines in Fig. 5 demarcate the lower and upper bounds T_{LB} and T_{UB} of the ASCE 7-22 period range of spectral fitting, for reference.

The governing demands generated by the MCE UHS target spectrum, demarcated by the horizontal black dotted lines in Fig. 5, exceed the largest governing demands generated by any of the 17 CMS targets for each of the three types of EDPs. In particular, the UHS demands of 2.64% drift, 42.1 MN base shear, and 1.27g roof acceleration exceed the maximum CMS demands of 1.95%, 36.3 MN, and 1.16g roof by approximately 35%, 16%, and 9%, respectively, as summarized in Table 3. The demands resulting from the theoretical CMS procedure also exceed the governing demands generated using a 75% UHS target spectrum ("UHS75"), which here is used as a proxy for the prescribed 75% lower bound of ASCE 7-22 criteria for CMS-based selection and is demarcated by horizontal gray dotted lines in Fig. 5. This degree of difference is slight for IDR_{max} and $V_{base,max}$, which are roughly 3-4% smaller using the UHS75 spectrum, and moderate for RA_{max} , which is about 14% smaller using UHS75. Also shown in Fig. 5 are correlation results (ρ) that will be discussed later.

3.2 Discussion

The EDP spectra of Fig. 5 demonstrate that the conditioning period T^* for which CMS demands are maximized varies depending upon the EDP. The T^* that maximizes the governing demand for IDR_{max} is 5s, which is equivalent to the fundamental period of the building, 4.22s, elongated by roughly 20%. In contrast, T^* of approximately 1s and 0.5s maximize governing demands for $V_{base,max}$ and RA_{max} , respectively, and fall relatively close to the building's lower-bound period $T_{LB} = 0.46s$ of the ASCE 7-22 period range for spectral fitting. Conditioning periods of 1s and 0.5s also closely coincide with the second and third natural periods of the structure listed in Table 1. Arteta et al. 2022 reported similar findings from performing exhaustive CMS-based nonlinear analysis on 16- and 24-story reinforced concrete moment frames subjected to 975- and 2475-year hazards. In particular, they found that for these structural archetypes and hazard levels, story drift,

base shear, and floor acceleration were each respectively maximized with T^* near to the elongated first-mode period, the second-mode period, and the third-mode period of each building. These results generally agree with known relationships between modal properties and building demands explained by structural dynamics. Whereas interstory drift is a largely first-mode-dominated phenomenon, story shear and floor acceleration are more sensitive to higher mode effects. Target spectra possessing relatively large spectral ordinates at one of these natural periods can amplify building excitation accordingly.

It is notable from the shape of the EDP spectrum of Fig. 5(a) that the IDR_{\max} estimates are relatively constant for a range of T^* near the maximizing value of $T^* = 5\text{s}$. Specifically, IDR_{\max} maintains at least 90% of the maximum value when $3\text{s} < T^* < 7\text{s}$. This corresponds to period values ranging from 0.6 to 1.4 times the maximizing value of $T^* = 5\text{s}$, which closely agrees with the analogous above-90% range for the 16- and 24-story buildings at the 975- and 2475-year hazard levels studied by Arteta et al 2022. In contrast with the results for drifts, we find the analogous gradients for $V_{\text{base,max}}$ and RA_{\max} are steeper, with the corresponding above-90% neighborhoods about the maximizing values of T^* being narrower ranges from 0.3s to 2s and 0.3s to 1s, respectively. These results indicate that exact precision in choice of T^* is not required to achieve building demands comparable to the maximum possible demands attained through rigorous CMS implementation. Nevertheless, story force- and floor acceleration-related demands appear to be somewhat more sensitive to choice of T^* than interstory drift-related demands for the studied building.

The observed elastic period elongation of primarily the first translational mode corroborates expectations expressed in the building code (ASCE, 2022), as well as those derived from industry experience. Some practitioners have reported first-period elongation on the order of 20% in tall buildings with core wall structural systems at the MCE ground motion level (e.g., J. Hooper, Magnusson Klemencic Associates, personal communication, 2021). The influence of period elongation on the EDP spectrum of IDR_{\max} was additionally confirmed by generating EDP spectra analogous to those of Fig. 5, but scaling down the 17 target spectra to 10% of their original spectral amplitudes (Fig. S2 of supplemental materials). In this case, with low structural nonlinearity, the range over which IDR_{\max} falls above 90% of the maximum value of 0.15% drift shifts lower to $1\text{s} < T^* < 5.5\text{s}$. This indicates that the increased degree of nonlinear behavior, stiffness degradation, and period elongation brought about by high ground motion intensity is reflected by rightward shifting of the peak interstory drift demands represented with an EDP spectrum.

We further elucidate the variation in EDP spectra with conditioning period by calculating the correlations between response spectral amplitudes at varying periods and the resulting amplitudes of building demands. Fig. 5 displays the values of these correlations as curves superimposed on the plots of the EDP spectra. As an illustrative example, the correlation coefficient $\rho_{IDR, Sa(T)}$ for IDR at $T = 3\text{s}$ is about 0.4 (Fig. 5(a)), which characterizes the linear dependence of the relationship between the natural logarithm of response spectral acceleration at $T = 3\text{s}$ and the natural logarithm of peak IDR demand, both corresponding to the same individual ground motion records. Pairs of $Sa(T = 3\text{s})$ values and peak IDR values were collected from all individual scaled records matched to all 17 of the CMS targets to calculate this correlation coefficient. The process was repeated for many closely spaced periods ranging from 0.15s to 9s and for the two other EDPs.

The general shapes of the correlation coefficient curves coincide well with the trends in the corresponding EDP spectra. The maximum values of ρ attained for IDR , V_{base} , and RA occur at periods of 5.35s, 1.05s, and 0.50s, respectively, which are close in value to the approximate EDP-maximizing CMS conditioning periods of 5s, 1s, and 0.5s. Though the periods of 5.35s and 5s pertaining to IDR are the furthest apart, the gradient of the EDP spectrum for IDR is relatively flat in this region, as previously noted, with the governing IDR demand decreasing by only about 3% from $T^* = 5\text{s}$ to $T^* = 6.33\text{s}$. It is thus reasonable to conclude from these results that the conditioning periods which maximize various types of EDPs are also those whose response spectral amplitudes have the highest correlation with the values of those EDPs. Put another way, these observations suggest that when sufficient individual analyses are performed, the correlation coefficient curves may be used as an approximate proxy of the shape of the EDP spectra, specifically the locations of maximum demands with respect to T^* .

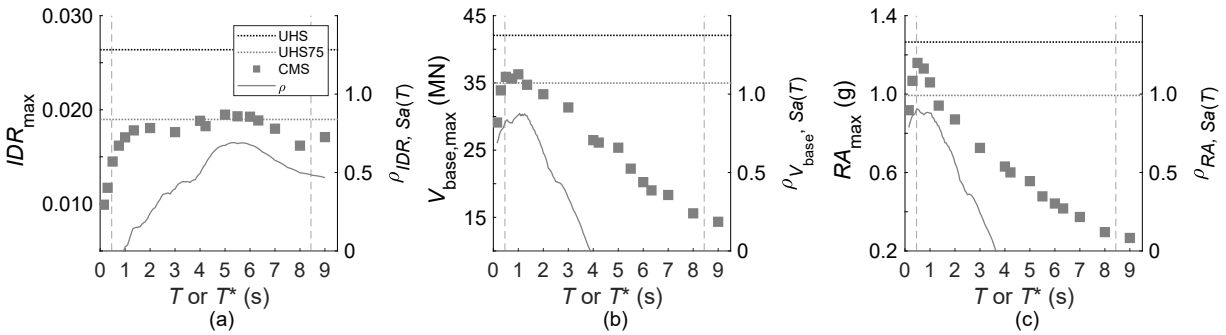


Fig. 5. EDP results of theoretical CMS procedure at MCE hazard level: (a) interstory drift ratio, (b) base shear, (c) roof acceleration. Values of EDP- $Sa(T)$ correlation coefficients superimposed.

4 Practical CMS Procedures

4.1 Results

Having established the demands generated for the building of study using a rigorous theoretical CMS procedure, we now examine the degree to which two practical approaches to CMS-based ground motion selection can recapture these results. The criteria of the two practical procedures examined, the ASCE 7-22 codified approach and an approach based on the recommendations of C&A-14, are summarized in the Introduction. The procedure described above for ground motion selection, nonlinear response history analysis, and calculation of buildings demands was performed for each individual target spectrum. In contrast with the theoretical CMS procedure, which used 17 distinct target spectra, we choose to use only two target spectra for each of the two practical CMS-based procedures. This constitutes the minimum number of targets required by ASCE 7-22 for CMS-based ground motion selection and is the typical number used in design practice. As numerous possible pairs of conditioning periods exist, we select three representative pairs of T^* to approximately bound the resulting demands and to illustrate their sensitivity to the choice of T^* . Fig. 4(b)-(c) show the three pairs of CMS-based target spectra corresponding to ASCE 7-22 and C&A-14, respectively. Results presented herein for these pairs of target spectra build on those of Bassman et al. (2022).

The first pair, {1s, 5s}, represents an idealized, preferred choice of T^* in which the selection of conditioning period is informed by a combination of the modal properties of the structure and estimation of period elongation. At the opposite extreme, the second pair, {0.15s, 9s}, constitutes a very poor choice of T^* that is included herein to approximately bound the results that can hypothetically be achieved using two target spectra. Lastly, the third pair, {3s, 8s}, represents one of many possible intermediate choices of T^* , both in terms of conditioning periods selected and quality of results, relative to the first two cases. This third case serves to help characterize the sensitivity of the resulting demands to perturbation of the chosen conditioning periods relative to the values of T^* which are known to maximize demands according to the EDP spectra of the theoretical CMS procedure.

All three pairs of target spectra constructed per C&A-14 were artificially modified to be in accordance with the recommendations of that paper. For the ASCE 7-22 targets, the {1s, 5s} pair required no artificial modifications to the original CMS, and the {3s, 8s} pair required only the left end of the CMS with $T^* = 3$ s be raised to meet the 75% UHS lower bound. The {0.15s, 9s} pair required both targets be raised in the region between the two conditioning periods. To meet the ASCE 7-22 criteria and also retain some consistency with the comparable C&A-14 targets, this pair was artificially raised symmetrically about the point halfway in log space between their respective conditioning periods, which is equivalent to the geometric mean of the two values of T^* .

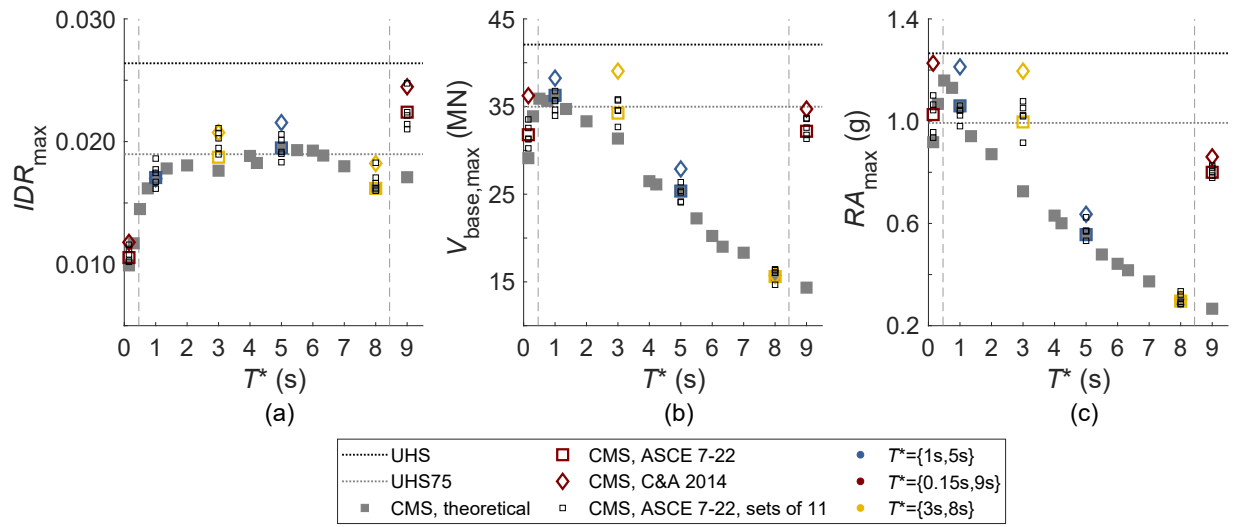


Fig. 6. Comparison of EDP results of theoretical and practical CMS procedures at MCE hazard level: (a) interstory drift ratio, (b) base shear, (c) roof acceleration.

Fig. 6 summarizes the governing demands produced by each of the practical procedures using each of the three pairs of targets, superimposing them on the EDP spectra of the theoretical CMS procedure from Fig. 5 for comparison. The large unfilled square markers correspond to the results of ASCE 7-22 and the unfilled diamond markers to those of C&A-14. Key building demands generated by the three procedures studied in this work and numerical comparisons between them are summarized in Table 3.

All of the aforementioned practical CMS-based analyses use 40 ground motions per spectral target, for consistency with prior results to obtain stable estimates of demands. However, as previously noted, ASCE 7-22 requires a minimum of only 11 records be selected per target. As such, in addition to the 40-record analysis conducted for each of the six individual targets across the three ASCE 7-22 target sets, five distinct 11-record analyses were performed for each target and their resulting governing demands plotted as smaller unfilled square markers in Fig. 6. The results of these additional analyses illustrate the variability in building demands which results when smaller but more commonly used 11-record sets are selected. Because the demand estimates based on 11-record sets can vary by $\sim 10 - 15\%$ or more, even with equivalent target spectra, changes to practical CMS procedures that only affect demands by a few percent are probably not of practical importance.

4.2 Discussion

The results of the ASCE 7-22 procedure using the preferred case of $T^*=\{1s, 5s\}$ corroborate those of the theoretical CMS procedure. The governing demands are similar to those of the theoretical CMS procedure, particularly for interstory drift and base shear. This outcome is reasonable as no modifications were required to the two original CMS, and these conditioning periods are those that maximized IDR_{max} and $V_{base,max}$ in the theoretical CMS procedure. With reference to Fig. 5, the value of T^* which maximizes $V_{base,max}$ (1s) is not the same as that which maximizes RA_{max} (0.5s), and the magnitudes of these two EDPs decrease relatively steeply away from their respective maxima. We observe that this discrepancy in maximizing T^* leads to an approximately 9% lower governing RA_{max} demand using ASCE 7-22, relative to that achieved using the theoretical CMS procedure. Though the degree of underestimation in this case is modest, it indicates the possibility for only a subset of all types of EDPs to be maximized simultaneously when an informed

Table 3. Summary comparison of governing demands resulting from the different ground motion selection procedures performed at the MCE hazard level.

| Demand or % Difference | IDR_{max} (%) | $V_{base,max}$ (MN) | RA_{max} (g) |
|--------------------------------|-----------------|---------------------|----------------|
| UHS | 2.64 | 42.1 | 1.27 |
| CMS Theoretical | 1.95 | 36.3 | 1.16 |
| % diff: UHS, CMS Theoretical | 35% | 16% | 9% |
| ASCE 7-22, $T^*=\{1s, 5s\}$ | 1.95 | 36.3 | 1.06 |
| C&A 2014, $T^*=\{1s, 5s\}$ | 2.15 | 38.2 | 1.21 |
| % diff: UHS, ASCE 7-22 | 35% | 16% | 19% |
| % diff: ASCE 7-22, CMS Theor. | 0.0% | 0.0% | -9% |
| % diff: C&A 2014, CMS Theor. | 11% | 5% | 5% |
| ASCE 7-22, $T^*=\{0.15s, 9s\}$ | 2.24 | 32.2 | 1.03 |
| C&A 2014, $T^*=\{0.15s, 9s\}$ | 2.45 | 36.2 | 1.23 |
| % diff: UHS, ASCE 7-22 | 18% | 31% | 23% |
| % diff: ASCE 7-22, CMS Theor. | 15% | -11% | -12% |
| % diff: C&A 2014, CMS Theor. | 26% | -0.1% | 6% |
| ASCE 7-22, $T^*=\{3s, 8s\}$ | 1.87 | 34.3 | 1.00 |
| C&A 2014, $T^*=\{3s, 8s\}$ | 2.07 | 39.0 | 1.20 |
| % diff: UHS, ASCE 7-22 | 41% | 23% | 27% |
| % diff: ASCE 7-22, CMS Theor. | -4% | -6% | -14% |
| % diff: C&A 2014, CMS Theor. | 6% | 8% | 3% |

selection of only two code-compliant target spectra is made. The degree to which one or more maximum demands may be missed depends on factors such as the gradient of the EDP spectrum with respect to T^* , which varies with the type of EDP and the hazard level, and the separation of modal periods, which depends on the building under consideration.

The other two cases of $\{0.15s, 9s\}$ and $\{3s, 8s\}$ underestimate the theoretical CMS procedure's results by a small to modest amount (4%-14%). The one exception to this trend is the governing IDR_{max} demand produced by the $\{0.15s, 9s\}$ set, which exceeds the theoretical CMS demand by 15%. While this discrepancy is conservative, it illustrates one unfavorable aspect of poorly chosen conditioning periods when only two target spectra are used and there is a large difference between their T^* , namely that a large artificial change to the target spectra may be needed to meet the 75% UHS lower bound. In this example, the $T^* = 9s$ target ends up with high spectral amplitudes over a wide range of periods, and this magnifies interstory drift-related demands.

The variation in demands between the theoretical procedure and the ASCE 7-22 procedure is generally comparable in magnitude to the variation in demands resulting from using sets of 11 ground motions instead of 40. For the $\{1s, 5s\}$ set, the demands achieved using sets of 11 records vary by -8% to 6% of the respective demand generated using 40 records, and by -9% to 11% and -8% to 13% for the $\{0.15s, 9s\}$ and $\{3s, 8s\}$ sets, respectively. These ranges are similar to those in Table 3 of -9% to 0%, -12% to 15%, and -14% to 4% which describe the difference between ASCE 7-22 results and theoretical results for the $\{1s, 5s\}$, $\{0.15s, 9s\}$, and $\{3s, 8s\}$ sets, respectively. In evaluating practical implementation of ground motion selection, effort expended to fine-tune target spectra via choice of conditioning periods and artificial modifications should be balanced against the impacts of other sources of uncertainty including the use of small sets of ground motion records, which may introduce comparable variability into the results.

The practical procedure based on C&A-14 produces governing demands for all three types of EDPs that are consistently greater than those produced using ASCE 7-22, as may be expected given the more

restrictive 90% UHS lower bound of the former procedure. The demands produced using C&A-14 are also greater than those produced using the theoretical CMS procedure by between 3% and 11%, with two exceptions: the governing value of $V_{\text{base,max}}$ in the {0.15s, 9s} target set is insignificantly (0.1%) lower than the theoretical CMS counterpart, and the governing value of IDR_{max} in this same target set is 26% greater than the theoretical CMS counterpart, for similar reasons as the analogous spectrum in the ASCE 7-22 {0.15s, 9s} target set. Hence, use of C&A-14 in this study provides a modest buffer of added conservatism over the results produced using ASCE 7-22, while also not exceeding UHS-based selection demands, as shown in Fig. 6.

Correlation coefficients between building demand amplitudes and response spectral amplitudes for the practical CMS procedures are shown in Fig. S3 in the supplemental materials, along with the correlation coefficient curves produced by the theoretical CMS procedure from Fig. 5 for comparison. Each of the new correlation curves was computed using only the results of the 80 total ground motion records selected for the corresponding pair of target spectra. Choice of either ASCE 7-22 or C&A-14 is observed to have minimal impact on the shape of the resulting correlation plot, while there is greater contrast between results for different choices of pairs of conditioning periods. Of note, all three pairs generally corroborate the locations of maximum correlations from the theoretical CMS procedure, even when the selected conditioning periods do not themselves coincide with the locations of these maxima. Closer qualitative agreement with the theoretical CMS correlations is achieved for the EDPs $V_{\text{base,max}}$ and RA_{max} , although the more gradual gradient of the EDP spectrum for IDR_{max} appears to be reflected in the greater spread in locations of maximum correlation across the three pairs of T^* . Additional noise is introduced to the correlation results when the number of ground motions selected per target spectrum is reduced from 40 to 11 motions (Figs. S4-S6 in the supplemental materials). These correlation coefficient curves may serve as one tool for validating the original choice of T^* when a reduced number of target spectra but sufficient numbers of ground motions are used, by comparing the periods at which the maximum correlations occur to the chosen conditioning periods.

5 Conclusions

This work has demonstrated that conditional mean spectrum (CMS)-based ground motion selection procedures that have been simplified for use in engineering practice are capable of considerably reducing the conservatism inherent to uniform hazard spectrum (UHS)-based selection while also remaining comparable in performance to theoretically rigorous CMS-based selection. Sets of only two CMS-based target spectra, with well-chosen conditioning periods (T^*), have been shown to reasonably reproduce drift, shear, and acceleration demands generated using an exhaustive set of 17 CMS targets for a tall building case study. Slight conservatism over the results of the exhaustive set is achieved when a sufficiently high floor on the envelope of the two target spectra is enforced, such as 90% of UHS, which slightly exceeds the current building code-minimum 75% of UHS.

This work also illustrates differences in how drift-, shear-, and acceleration-related engineering demand parameters (EDPs) vary with respect to changes in T^* of the CMS target spectra. We have demonstrated that EDP spectra, which plot maximum EDPs against T^* of the corresponding CMS targets, are a useful and concise visual tool for analyzing the effects of choice of T^* as well as period elongation under nonlinear behavior on resulting building demands. At the MCE hazard level for the case study building, interstory drifts were maximized using an elongated first-mode elastic period for T^* , whereas base shear and roof acceleration were maximized when T^* was respectively equal to the second and third elastic modes. The magnitudes of drift demands changed more slowly with varied T^* than the other two types of EDPs; 90% of the theoretical maximum drift demand could be maintained within about $\pm 2s$ of the maximizing T^* , whereas this range was $\pm 1s$ or narrower for the other two EDPs.

For high-rise structures similar to the building in this study, these EDP results demonstrate that accounting for nonlinear-response-related elongation in fundamental period in the choice of conditioning period has minor impact on the governing interstory drift ratio and provides decreased base shear and roof acceleration demands. Based on the results of the tall building analyzed in this study, it is suggested that an initial selection of conditioning periods for similar tall buildings include the 20%-elongated fundamental period(s) of the structure, as well as the second and possibly third elastic mode periods depending on their modal separation. Further study of other tall building archetypes will inform the broader applicability of these findings.

In practice, due attention should be paid to other prominent sources of uncertainty in the building demands resulting from the analysis, particularly the number of ground motions used. The code-minimum 11 records per target spectrum was found in this study to introduce comparable variability into the resulting demands, meaning that precise choice of T^* may often have a smaller effect on the results than inherent variability caused by randomness in the ground motion set.

One means of checking the aptitude of the chosen values of T^* after dynamic structural analysis has been performed is to calculate correlation coefficients between response spectral amplitudes and EDP amplitudes, which can be visually superimposed on EDP spectra. We have shown that the periods at which these correlations are maximized are approximately the values of T^* that maximize the corresponding EDPs.

These findings are based on a refined model for a class of buildings that is commonly assessed using CMS, so the presented results are relevant for a number of practical situations. Further, the findings are consistent with general concepts from structural dynamics and ground motion characterization, suggesting that similar results are likely to be seen in other cases. Future analyses of this nature for other types of engineering demand parameters and structures, and using refined models that incorporate three-dimensional effects, could further broaden these findings. Ground motion metrics beyond response spectra, such as shaking duration, could also be incorporated using a similar approach (Bradley, 2012; Raghunandan and Liel, 2013; Chandramohan et al., 2016). If explicit evaluation of simplified CMS procedures is desired for some other structural system or analysis case, this paper presents a general procedure that could be replicated for further study of those cases.

6 Data Availability Statement

Some or all data, models, or code generated or used during the study are available in a repository online (Bassman, 2022).

7 Acknowledgements

The authors thank Stanford University and the Stanford Research Computing Center for providing high-performance computing resources on the Sherlock cluster that were used for running structural analysis. Thanks to Peter Powers, Sanaz Rezaeian, and Nicolas Luco at the USGS for providing seismic hazard disaggregation data. Thanks to John Hooper and the team at Magnusson Klemencic Associates as well as two anonymous reviewers for insightful comments and discussion that improved the quality of this paper.

8 Supplemental Materials

Tables S1-S2 and Figs. S1-S6 are available online in the ASCE Library (ascelibrary.org).

References

- Arteta, C. A., Torregroza, A., Gaspar, D., and Abrahamson, N. (in press, 2022). "Sensitivity of the conditional period selection in the structural response using the cms as target spectrum." *Earthquake Spectra*.
- ASCE (2022). *Minimum Design Loads and Associated Criteria for Buildings and Other Structures*, ASCE 7-22. Number ASCE/SEI 7-22. American Society of Civil Engineers/Structural Engineering Institute, Reston, Virginia.
- Baker, J. W. (2011). "Conditional mean spectrum: Tool for ground motion selection." *Journal of Structural Engineering*, 137(3), 322–331.
- Baker, J. W. and Cornell, C. A. (2006). "Spectral shape, epsilon and record selection." *Earthquake Engineering & Structural Dynamics*, 35(9), 1077–1095.
- Baker, J. W. and Jayaram, N. (2008). "Correlation of spectral acceleration values from nga ground motion models." *Earthquake Spectra*, 24(1), 299–317.
- Baker, J. W. and Lee, C. (2018). "An improved algorithm for selecting ground motions to match a conditional spectrum." *Journal of Earthquake Engineering*, 22(4), 708–723.
- Bassman, T. J. (2022). "Conditional mean spectra code criteria evaluation, <10.5281/zenodo.6510435> (1).
- Bassman, T. J., Zhong, K., and Baker, J. W. (2022). "Ground motion selection using code-compliant conditional mean spectra: Effects of conditioning period and amplitude constraints." *Proceedings of the 12th National Conference on Earthquake Engineering*, Earthquake Engineering Research Institute.
- Boore, D. M., Stewart, J. P., Seyhan, E., and Atkinson, G. M. (2014). "Nga-west2 equations for predicting pga, pgv, and 5% damped psa for shallow crustal earthquakes." *Earthquake Spectra*, 30(3), 1057–1085.
- Bozorgnia, Y., Abrahamson, N. A., Atik, L. A., Ancheta, T. D., Atkinson, G. M., Baker, J. W., Baltay, A., Boore, D. M., Campbell, K. W., Chiou, B. S.-J., Darragh, R., Day, S., Donahue, J., Graves, R. W., Gregor, N., Hanks, T., Idriss, I., Kamai, R., Kishida, T., Kottke, A., Mahin, S. A., Rezaeian, S., Rowshandel, B., Seyhan, E., Shahi, S., Shantz, T., Silva, W., Spudich, P., Stewart, J. P., Watson-Lamprey, J., Wooddell, K., and Youngs, R. (2014). "Nga-west2 research project." *Earthquake Spectra*, 30(3), 973–987.
- Bradley, B. A. (2012). "A ground motion selection algorithm based on the generalized conditional intensity measure approach." *Soil Dynamics and Earthquake Engineering*, 40, 48–61.
- Carlton, B. and Abrahamson, N. (2014). "Issues and approaches for implementing conditional mean spectra in practice." *Bulletin of the Seismological Society of America*, 104(1), 503–512.
- Chandramohan, R., Baker, J. W., and Deierlein, G. G. (2016). "Impact of hazard-consistent ground motion duration in structural collapse risk assessment." *Earthquake Engineering & Structural Dynamics*, 45(8), 1357–1379.
- Christie, S. R. and Zhang, Y. (2016). "Seismic design of the new elliott bay seawall using the conditional mean spectrum." *Ports 2016*, 152–161.
- Du, W., Ning, C.-L., and Wang, G. (2019). "The effect of amplitude scaling limits on conditional spectrum-based ground motion selection." *Earthquake Engineering & Structural Dynamics*, 48(9), 1030–1044.

- Gregor, N., Abrahamson, N. A., Atkinson, G. M., Boore, D. M., Bozorgnia, Y., Campbell, K. W., Chiou, B. S.-J., Idriss, I. M., Kamai, R., Seyhan, E., Silva, W., Stewart, J. P., and Youngs, R. (2014). "Comparison of nga-west2 gmpes." *Earthquake Spectra*, 30(3), 1179–1197.
- Hashash, Y. M. A., Abrahamson, N. A., Olson, S. M., Hague, S., and Kim, B. (2013). "Conditional mean spectra in site-specific seismic hazard evaluation for a major river crossing in the central united states." *Earthquake Spectra*, 31(1), 47–69.
- Kishida, T. (2017). "Conditional mean spectra given a vector of spectral accelerations at multiple periods." *Earthquake Spectra*, 33(2), 469–479.
- Kwong, N. S. and Chopra, A. K. (2017). "A generalized conditional mean spectrum and its application for intensity-based assessments of seismic demands." *Earthquake Spectra*, 33(1), 123–143.
- LATBSDC (2020). *An Alternative Procedure for Seismic Analysis and Design of Tall Buildings Located in the Los Angeles Region*. Los Angeles Tall Buildings Structural Design Council Los Angeles, CA.
- Loth, C. (2014). *Multivariate Ground Motion Intensity Measure Models, and Implications for Structural Reliability Assessment*. Dept. of Civil and Environmental Engineering. Stanford University, Stanford, CA.
- Loth, C. and Baker, J. W. (2015). "Rational design spectra for structural reliability assessment using the response spectrum method." *Earthquake Spectra*, 31(4), 2007–2026.
- McKenna, F., Scott, M. H., and Fenves, G. L. (2010). "Nonlinear finite-element analysis software architecture using object composition." *Journal of Computing in Civil Engineering*, 24(1), 95–107.
- Moehle, J., Bozorgnia, Y., Jayaram, N., Jones, P., Rahnama, M., Shome, N., Tuna, Z., Wallace, J., Yang, T., and Zareian, F. (2011). "Case studies of the seismic performance of tall buildings designed by alternative means." *Pacific Earthquake Engineering Research Center College of Engineering University of California, Berkeley PEER Report*, 5.
- Moehle, J. P., Hamburger, R. O., Baker, J. W., Bray, J. D., Crouse, C. B., Deierlein, G. G., Hooper, J. D., Lew, M., Maffei, J. R., Mahin, S. A., Malley, J., Naeim, F., Stewart, J. P., and Wallace, J. W. (2017). "Guidelines for performance-based seismic design of tall buildings version 2.0." *Report No. PEER Report 2017/06*, Berkeley, CA.
- Petersen, M. D., Moschetti, M. P., Powers, P. M., Mueller, C. S., Haller, K. M., Frankel, A. D., Zeng, Y., Rezaeian, S., Harmsen, S. C., Boyd, O. S., Field, N., Chen, R., Rukstales, K. S., Luco, N., Wheeler, R. L., Williams, R. A., and Olsen, A. H. (2015). "The 2014 united states national seismic hazard model." *Earthquake Spectra*, 31(1_suppl), S1–S30.
- Raghunandan, M. and Liel, A. B. (2013). "Effect of ground motion duration on earthquake-induced structural collapse." *Structural Safety*, 41, 119–133.
- Zhong, K., Lin, T., Deierlein, G. G., Graves, R. W., Silva, F., and Luco, N. (2021). "Tall building performance-based seismic design using sceec broadband platform site-specific ground motion simulations." *Earthquake Engineering & Structural Dynamics*, 50(1), 81–98.